RSC Advances

PAPER

Cite this: *RSC Adv.*, 2020, **10**, 31800

A comparative study of the structures, thermal stabilities and energetic performances of two energetic regioisomers: 3(4)-(4-aminofurazan-3-yl)-4(3)-(4-nitrofurazan-3-yl)furoxan†

Jiarong Zhang,[ac] Fuqiang Bi,*[bc] Lianjie Zhai,[c] Huan Huo,[c] Zhi Yang[a] and Bozhou Wang*[c]

Although energetic regioisomers have attracted intensive attention due to their interesting structure–property correlation, their effective synthesis and accurate identification has remained very difficult. In this paper, we synthesized two energetic regioisomers, namely 3-(4-aminofurazan-3-yl)-4-(4-nitrofurazan-3-yl)furoxan (ANFF-34) and 4-(4-aminofurazan-3-yl)-3-(4-nitrofurazan-3-yl)furoxan (ANFF-43), *via* a controllable strategy with improved yields of 32% and 38%, respectively. The structures of ANFF-34 and ANFF-43 were unambiguously identified using comparative studies of ^{15}N NMR and single-crystal X-ray diffraction. Moreover, their thermal behaviours, and non-isothermal thermodynamic parameters were systematically investigated. Both ANFF-34 (T_m: 116.2 °C, T_d: 255.4 °C) and ANFF-43 (T_m: 106.2 °C, T_d: 255.6 °C) have similar thermal decomposition processes to that of DNTF. The superior performances of ANFF-34 (ρ: 1.8 g cm^{-3}, D: 8214 m s^{-1}, P: 30.5 GPa, IS > 40 J) and ANFF-43 (ρ: 1.7 g cm^{-3}, D: 7868 m s^{-1}, P: 27.0 GPa, IS > 40 J) indicate their great potential to be used as melt-cast carrier explosives. This study provides a solid foundation for the design and synthesis of new energetic compounds through isomer effects.

Received 16th July 2020
Accepted 11th August 2020

DOI: 10.1039/d0ra06186g

rsc.li/rsc-advances

Introduction

The search for new melt-cast explosives with satisfactory comprehensive performances represents an important topic in the field of energetic materials, owing to their wide application in weapon systems.[1] Over the years, many nitro heterocyclic compounds such as MDNI,[2] MDNT,[3] TNAZ,[4] and DNTF[5] have been synthesized as melt-cast energetic materials. Among them, DNTF represents a desired melt-cast explosive, due to its high density of 1.93 g cm^{-3}, high detonation velocity of 9250 m s^{-1}, positive heat of formation of 657 kJ mol^{-1} (ref. 6) and satisfactory melting point of 108–110 °C.[7] The high nitrogen content and positive enthalpy of formation resulting from its bisfurzanylfuroxan backbone contribute significantly to the high energy of DNTF. However, DNTF is sensitive to impact and there are still many security issues needing to be addressed for its practical applications. According to the research consensus in the field of insensitive energetic materials, the introduction of hydrogen bonds within or between nitrogen-rich aromatic heterocycles is an effective strategy to reduce the sensitivity of energetic materials to external stimuli.[8] Therefore, based on the bisfurzanylfuroxan backbone of DNTF, the replacement of one nitro by an amino in DNTF will greatly reduce its sensitivity.

The energetic compounds based on the furoxan structure usually possess regioisomers, due to the different positions of N-oxide[9] (Scheme 1). Indeed the arrangement of functional groups significantly affects the performances of derived energetic materials. A thorough understanding of the correlation between structures and performances of isomeric energetic compounds is of significant importance in terms of designing and synthesizing new energetic compounds using isomer effects. However, there are only few reports on the relationship between the structure and properties of energetic isomers by far.

In 2012, T. K. Kim *et al.*[10] reported the synthesis of 4-(4-aminofurazan-3-yl)-3-(4-nitrofurazan-3-yl)furoxan (ANFF-43) based on the backbone of bisfurzanylfuroxan. In 2017, R. Duddu[7] *et al.* reported the synthesis of ANFF-43 and its regioisomer 3-(4-aminofurazan-3-yl)-4-(4-nitrofurazan-3-yl) furoxan (ANFF-34) with yields of less than 10%. The melting

[a]*School of Chemistry and Chemical Engineering, Beijing Institute of Technology, Beijing, 100081, PR China*

[b]*Key Laboratory of Applied Surface and Colloid Chemistry, MOE/School of Chemistry and Chemical Engineering, Shaanxi Normal University, Xi'an 710062, PR China. E-mail: bifuqiang@gmail.com*

[c]*Xi'an Modern Chemistry Research Institute, Xi'an 710065, PR China. E-mail: wbz600@163.com*

† Electronic supplementary information (ESI) available. CCDC 2012931 and 2012930. For ESI and crystallographic data in CIF or other electronic format see DOI: 10.1039/d0ra06186g

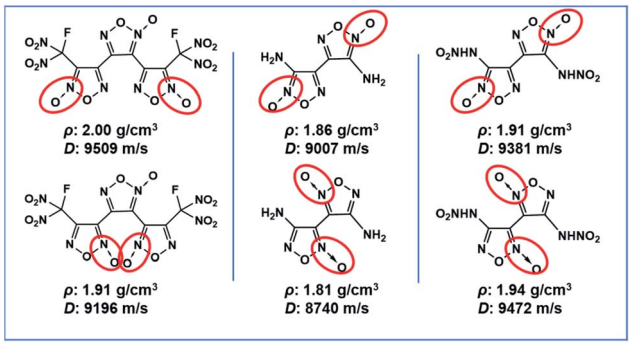

Scheme 1 Reported regiochemical energetic materials with different performances.

points of ANFF-34 and ANFF-43 are 116.2 °C and 106.2 °C, respectively, indicating great potential to be used as melt-cast explosives. Unfortunately, their structural characterization conclusions were contradictory, and the detonation performances of the two compounds were not reported. Moreover, the impacts of structures on the performances of ANFF-34 and ANFF-43 were not explored.

In order to clearly identify the structures of ANFF-43 and ANFF-34 and explore the relationship between the structures and performances of furoxanyl-isomer compounds, we synthesized ANFF-34 and ANFF-43 using DNTF as the starting material, through a controllable strategy with improved yields. Their structures were unambiguously identified by establishing the correlation between the theoretical ^{15}N NMR chemical shift value and the experimental value, and cultivating the single crystals of the two compounds. Indeed, this is the first time that the single crystal of ANFF-43 was obtained. Moreover, the thermal behaviours, non-isothermal thermodynamic parameters, sensitivities and detonation performances of ANFF-34 and ANFF-43 were systematically investigated.

Experiment

General caution! Although we have experienced no explosion accident in synthesis and characterization of these materials, proper protective measures should be adopted.

Materials and instruments

DNTF used in this study was supplied by Xi'an Modern Chemistry Research Institute. $NH_3 \cdot H_2O$ (25–28% NH_3 in water) and other reagents were commercially available and used without further purification. ^{1}H NMR, ^{13}C NMR and ^{15}N NMR spectra of ANFF-34 and ANFF-43 were recorded on 500 MHz (Bruker AVANCE 500) nuclear magnetic resonance spectrometers. The samples were dissolved in solvent DMSO-d_6. The melting and decomposition points were determined using a differential scanning calorimeter (TA Instruments Company, Model DSC-Q200) at a flow rate of N_2 at 50 mL min^{-1}. About 0.5 mg of the sample was sealed in aluminium pans for DSC analysis. Infrared spectra were obtained from KBr pellets on a Nicolet NEXUS870 Infrared spectrometer in the range of 4000–400 cm^{-1}. Elemental analysis (C, H and N) were performed on a VARI-El-3 elementary analysis instrument. The impact and friction sensitivities were determined using the BAM method.

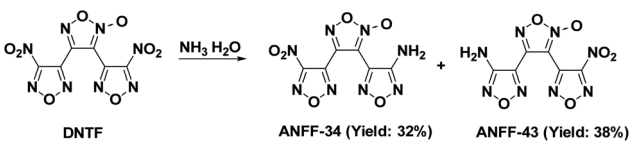

Scheme 2 The synthesis approach of ANFF-34 and ANFF-43.

X-ray crystallography

The diffraction data of ANFF-34 and ANFF-43 were collected on a BRUKER SMART Apex II CCD X-ray diffractometer equipped with a Mo Kα radiation (λ = 0.71073 A) using ω–θ scan mode. The structures were solved by the direct method using SHELXS-97 and refined with full-matrix least-squares procedures on F^2 with SHELXL-97. The crystal data and structure refinement parameters were listed in Tables S1 and S2.† The selected bond lengths, bond angles and hydrogen bond data were summarized in Tables S3–S6.† The crystal structures of ANFF-34 and ANFF-43 have been deposited with the Cambridge Crystallographic Data Centre (CCDC), under deposition numbers 2012930 and 2012931.†

Synthetic procedures

Under −10 °C, 10 mL $NH_3 \cdot H_2O$ was added to DNTF (3.1 g, 10 mmol) with stirring and the solution was maintained at room temperature for 4–6 hours until DNTF was completely consumed (monitored by TCL). After the solvent was removed under reduced pressure, the crude product was separated using silica gel column chromatography with gradient elution consisting of ethyl acetate and petroleum ether. 0.9 g ANFF-34 was obtained as white solid with a yield of 32%. T_m = 116.2 °C, $T_{dec\ (peak)}$ = 255.4 °C. IR (KBr): $\tilde{\nu}$ = 3489, 3389, 1642, 1563, 1520, 1462, 1430, 1401, 1359, 1312, 1283, 1171, 1145, 999, 960, 831, 807; ^{1}H NMR (500 MHz, DMSO-d_6): δ ppm: 6.54 (s, 2H, NH_2); ^{13}C

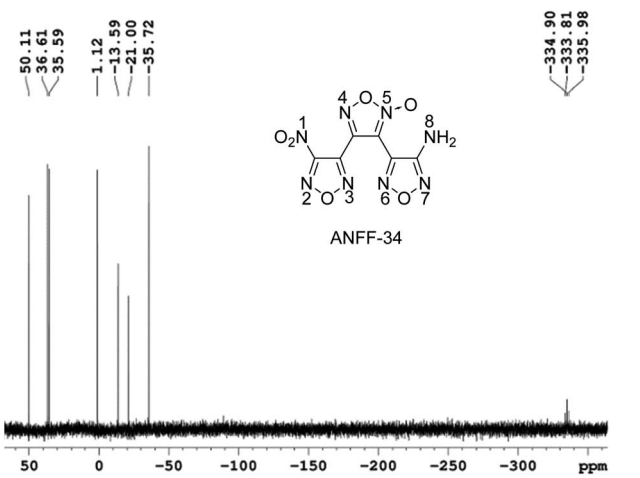

Fig. 1 The experimental ^{15}N NMR spectrum of ANFF-34.

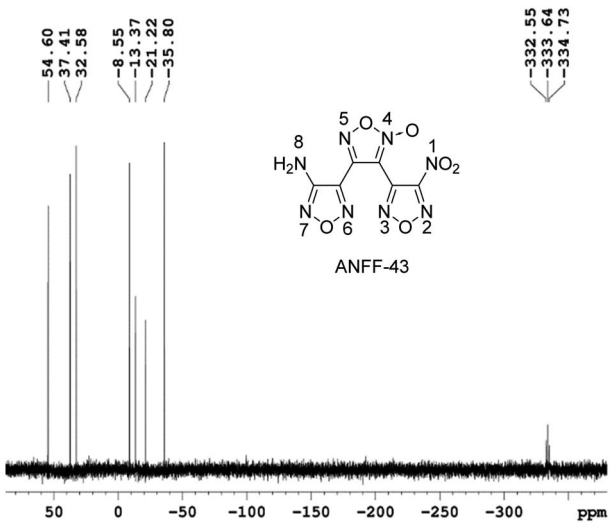

Fig. 2 The as-recorded ^{15}N NMR spectrum of ANFF-43.

NMR (125 MHz, DMSO-d_6): δ ppm: 106.13, 133.43, 139.63, 143.06, 155.81, 159.79; ^{15}N NMR (125 MHz, DMSO-d_6): δ ppm: −333.81, −35.72, −21.00, −13.59, 1.12, 35.59, 36.61, 50.11; elemental analysis calculated (%) for $C_6H_2N_8O_6$: C 25.49, H 0.70, N 39.75; found: C 25.52, H 0.72, N 39.70.

1.1 g ANFF-43 was obtained as white solid with a yield of 38%. T_m = 106.2 °C, $T_{dec\ (peak)}$ = 255.6 °C. IR (KBr): $\tilde{\nu}$ = 3470; 3342; 1637; 1597; 1561; 1510; 1467; 1408; 1358; 1289; 1122; 996; 965; 830, 810; ^{1}H NMR (500 MHz, DMSO-d_6): δ ppm: 6.71 (s, 2H, NH_2); ^{13}C NMR (125 MHz, DMSO-d_6): δ ppm: 102.08; 136.29; 137.34; 145.93; 155.13; 159.95; ^{15}N NMR (125 MHz, DMSO-d_6): δ ppm: −333.64; −35.80; −21.22; −13.37; −8.55; 32.58; 37.41; 54.60; elemental analysis calculated (%) for $C_6H_2N_8O_6$: C 25.49, H 0.70, N 39.75; found: C 25.51, H 0.72, N 39.79.

Results and discussion

Controllable synthesis

2012, T. K. Kim[10] and co-workers synthesized ANFF-43 with a yield of 30.1%. 2017, R. Duddu[7] *et al.* adopted diamino furazanofuroxan (DAFF) as starting material, synthesized ANFF-34 and ANFF-43 with low yields of 8.4% and 6.9%, respectively. Herein, we synthesized these two materials based on nucleophilic displacement reaction between $NH_3 \cdot H_2O$ and the nitro group of DNTF, we commenced the experiment under −10 °C to avoid over substitution of nitro groups. Under the carefully controlled synthesis condition, the reactivity of NH_3 was effectively reduced, and only one –NH_2 substituted products (ANFF-34 and ANFF-43) were obtained successfully with improved yields of 32% and 38% (Scheme 2).

Structure analysis

Isomers possess same molecular formula and elements and similar configurations, but the slight difference in structure usually has a remarkable impact on its performances. Hence, the confirmation of their structure is crucial, but very challenging in organic synthesis. It is noteworthy herein that the clarification of the structures of ANFF-34 and ANFF-43 and investigation on the relationship between structure and performances have great academic significance, for the design and synthesis of energetic materials with isomeric characters.

As mentioned above, R. Duddu obtained the crystal structure of ANFF-34 and deduced the NMR assignment of ANFF-43, then pointed out that "we conclude that Chung and co-workers have indeed obtained 6 (ANFF-34) but erroneously assigned their isolated compound's structure as 7 (ANFF-43)".

These controversial results have attracted our attention when we tried to determine the structures of ANFF-34 and ANFF-43. Using nitromethane as an external standard, the ^{15}N NMR spectra of ANFF-34 and ANFF-43 were recorded, and the chemical shifts were given in Fig. 1 and 2. In order to identify the structures, we further calculated the ^{15}N NMR displacement information of ANFF-34 and ANFF-43, based on the B3LYP/6-311+G (2d, p) method by using Gaussian 09 program. The calculated chemical shifts are the simulated value of the compounds in ideal gas state, therefore, they are different from the experimental chemical shifts. We analyzed the linear correlation coefficients between the theoretical value and experimental value, and the results of ANFF-34 and ANFF-43 are greater than 99.8%, indicating the change trends of the calculated and experimental results are very consistent. Therefore,

Table 1 The experimental and calculated chemical shifts of ^{15}N NMR of ANFF-34 and ANFF-43

	ANFF-34		ANFF-43	
N number	Experimental	Calculated	Experimental	Calculated
N8	−333.81	−357.31	−333.64	−357.26
N7	−13.59	3.51	−8.55	1.75
N6	35.59	45.82	32.58	44.98
N5	−21.00	−20.29	−21.22	−15.19
N4	1.12	11.66	−13.37	−14.3
N3	50.11	70.10	54.60	73.37
N2	36.61	59.67	37.41	61.21
N1	−35.72	−29.52	−35.8	−29.21
Correlation coefficient	$y = 1.1092x + 11.871$, $R^2 = 0.9984$		$y = 1.1078x + 10.547$, $R^2 = 0.9985$	

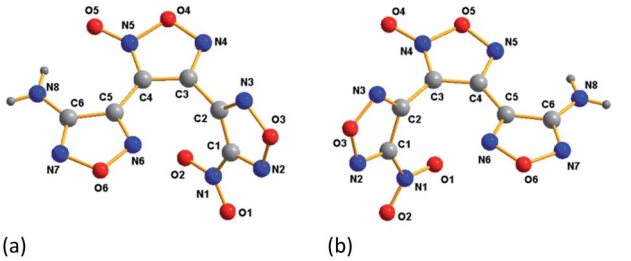

Fig. 3 Single-crystal X-ray structures of compounds ANFF-34 (a) and ANFF-43 (b).

the structures of ANFF-34 and ANFF-43 were clearly identified (Table 1).

Surprisingly, the IR spectrum and ^{13}C NMR of ANFF-43 were basically consistent with the data reported by T. K. Kim, while they were inconsistent with the data reported by R. Duddu. In order to accurately identify the structures of the two isomers, we further cultivated the crystal of the two compounds. Suitable crystals of ANFF-34 and ANFF-43 were obtained by slow evaporation of petroleum ether/ethyl acetate solution at room temperature.

ANFF-34 crystalizes in the monoclinic space group $P2(1)/n$ with four molecules per unit one cell. As illustrated in Fig. 3a, the aminofurazan ring and the furoxan ring are basically in the same plane, and the dihedral angle between the nitrofurazan ring and the furoxan ring is 65.34°. The bond length of N5–O5 is 1.222 Å, which is shorter than the average value of typical N–O distance (1.40 Å) and very close to that of N=O double bond. In the presence of N8–H–O2 intermolecular hydrogen bonds and N8–H–O5 intramolecular hydrogen bonds, ANFF-34 exists as a "face-to-face" dimer formation in the crystal (Fig. 4a). ANFF-34 possesses a density of 1.80 g cm^{-3}, which is higher than that of ANFF-43. From the in-depth analysis of the crystal structure of

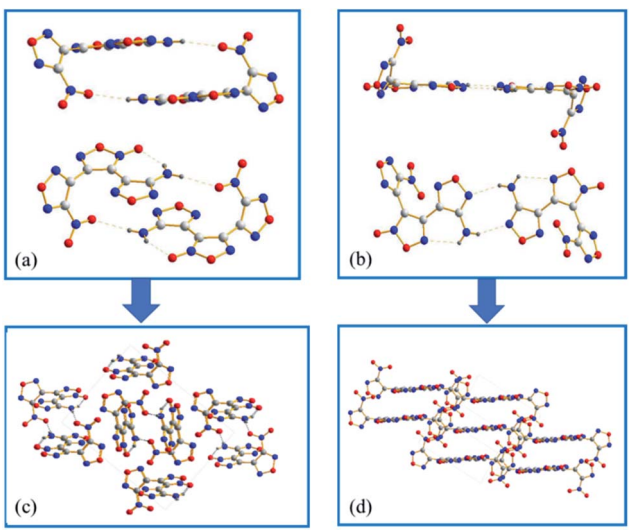

Fig. 4 (a) The face-to-face dimer formation of ANFF-34; (b) the hand-in-hand dimer formation of ANFF-43; (c) 3D stacking diagram of ANFF-34. (d) 3D stacking diagram of ANFF-43.

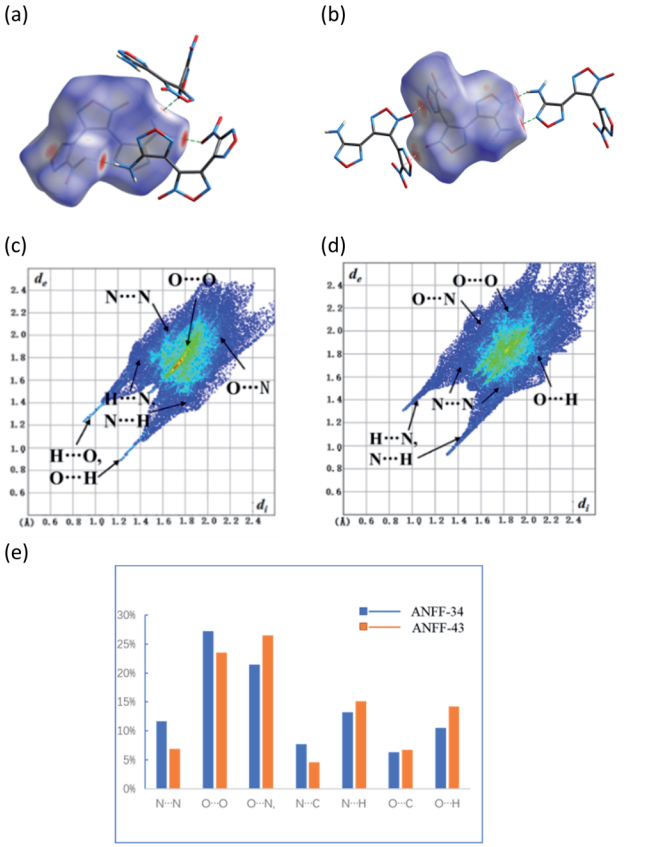

Fig. 5 (a) Hirshfeld surface of ANFF-34; (b) Hirshfeld surface of ANFF-43; (c) 2D fingerprint plot of ANFF-34; (d) 2D fingerprint plot of ANFF-43; (e) comparison of the amounts of close interactions in ANFF-34 and ANFF-43.

the two isomers, it is reasonable to deduce that the high density of ANFF-34 is because its dimer formation is closer, which promotes its 3D structure to be more densely packed (Fig. 4c).

ANFF-43 crystalizes in the triclinic space group $P\bar{1}$ with two molecules per unit one cell at 296 K. The aminofurazan ring and the furoxan ring are also in the same plane (Fig. 3b), while the dihedral angle between the nitrofurazan ring and the central

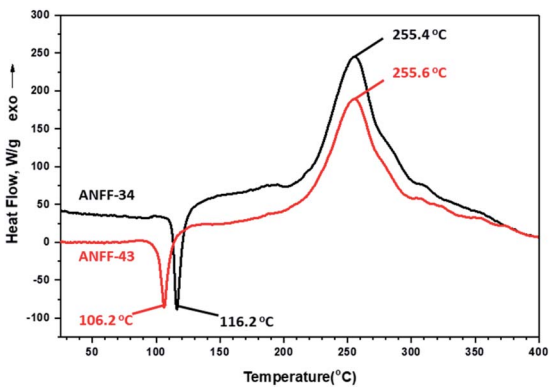

Fig. 6 The DSC traces of ANFF-34 and ANFF-43.

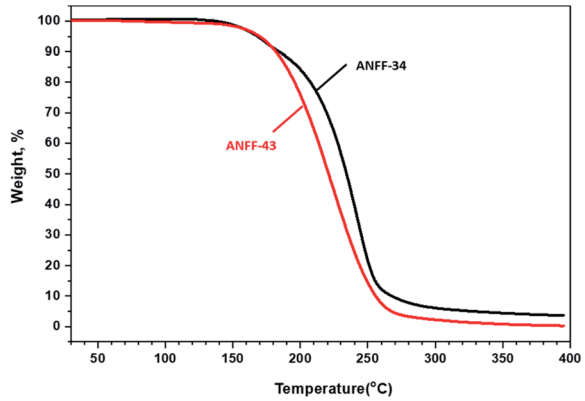

Fig. 7 The TG traces of ANFF-34 and ANFF-43.

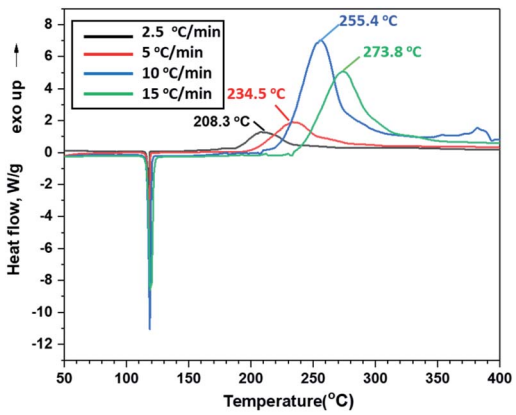

Fig. 8 DSC traces of ANFF-34 obtained at various heating rates.

furoxan ring is 63.42°. Unlike ANFF-34, the crystal density of ANFF-43 is only 1.70 g cm^{-3}, significantly lower than that of ANFF-34. There are also intermolecular hydrogen bonds N8–H–N6 and intramolecular hydrogen bonds N8–H–N5 in the crystal, making ANFF-43 exists as a "hand-in-hand" dimer formation (Fig. 4b). As expected, this kind of dimer configuration renders

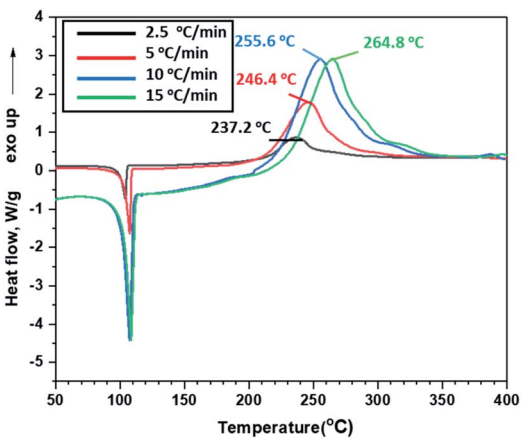

Fig. 9 DSC traces of ANFF-43 obtained at various heating rates.

the 3D structure of ANFF-43 loose and its density lower than that of ANFF-34 (Fig. 4d). It is noteworthy that all the lengths of the bonds in ANFF-34 are slightly shorter than those of ANFF-43 (except N–H bond in the amino group), indicating that ANFF-34 possesses a more compact structure. The detailed crystal structure analysis clearly indicates how the regiochemical modification affects the structure of ANFF-34 and ANFF-43 and the resulting differences in their performances.

The bond lengths of the three furazan in DNTF are similar to that of the standard furazan bonds (Table S7†), so each of them constitutes a stable conjugated system. From the crystal packing diagram of DNTF (Fig. S6†), the three furazan rings in DNTF molecule are in three different planes, and form a stable chair-shaped structure in space, which makes the molecules pack more tightly, thus DNTF exhibits a higher density of 1.937 g cm^{-3}.

The included angles of the three furazan rings in the two nitro reduction products 3,4-diaminofurazanofuroxan (DAFF) (Fig. S10†) are 40.33° and 13.75°, respectively, indicating that the three furazan rings are twisted, and the compound has no aromaticity. It can be seen from Fig. S11† that the distorted DAFF molecules are arranged in a disorderly manner in the crystal, which makes DAFF molecules loosely packed, and finally lead to the low density of the DAFF (1.745 g cm^{-3}).

Hirshfeld analysis

The Hirshfeld surfaces (d_{norm}) of ANFF-34 and ANFF-43 were calculated by CrystalExplorer[11] and shown in Fig. 5a and b. The 3D d_{norm} surface was used to identify close intermolecular interactions. The red and blue regions represent longer and closer contacts, and the white regions represent the distance of contacts equal to exactly the vdW separation with a d_{norm} value of zero. The red dots appeared on the surfaces of ANFF-34 and ANFF-43 are mainly resulted from intermolecular hydrogen bonds, which make them exist as "face-to-face" and "hand-in-hand" dimer formation, respectively. The red areas attributed to hydrogen bonds are dark, indicating the presence of strong hydrogen bonds. In comparison with ANFF-43, ANFF-34 possesses more "hot spots" in its crystal structure, leading to its increased sensitivities and reduced safety.

The 2D fingerprint plots clearly illustrate the contributions of intermolecular interactions (Fig. 5c and d). It has been reported that the O···H and N···H interactions help to decrease the sensitivities, while the O···O interactions usually increase the sensitivity of a compound.[9] As shown in Fig. 5e, O···O contact interaction of ANFF-34 accounts for 27.2% of the total weak interactions, which is higher than that of ANFF-43 (23.5%). In contrast, the O···H contact interaction of ANFF-34 (10.5%) are lower than that of ANFF-43 (14.2%). We found that the content of O···O bonds in DNTF is up to 34.9% (Fig. S9†), and there are no O···H and N···H interactions in DNTF, so DNTF shows more sensitivities to impact (26 J) and friction (240 N). These results indicate that ANFF-34 is more sensitive to external mechanical stimuli than ANFF-43, which is in good consistency with the crystal analysis and experimental results.

Table 2 Kinetic parameters and enthalpies of thermal decomposition of ANFF-34 and ANFF-43[a]

	β_i (K min^{-1})	T_i (K)	E_k (kJ mol^{-1})	r	lg A_k (s^{-1})
ANFF-34	2.5	481.4	52.22	0.991	10.34
	5	507.7			
	10	528.5			
	15	546.9			
ANFF-43	2.5	510.3	142.1	0.989	13.77
	5	519.5			
	10	528.7			
	15	537.9			

[a] E_k is the apparent activation energy; r is the liner correlation coefficient; A_k is pre-exponential factor.

Thermal behaviour

Thermal behaviours of ANFF-34 and ANFF-43 were investigated and compared by DSC-TG under a heating rate of 10 °C min^{-1} in N_2 atmosphere (Fig. 6 and 7). From Fig. 6, ANFF-34 and ANFF-43 have similar thermal decomposition processes, and both melt first and then decompose. The melting point of ANFF-43 is 106.2 °C which is lower than that of ANFF-34 (116.2 °C), but the thermal decomposition peak temperatures of the two compounds are very close (255.4 °C and 255.6 °C). The result shows that both ANFF-34 and ANFF-43 hold great potential to be used as melt cast explosives, and possess good thermal stabilities which are similar to that of DNTF (T_m: 110 °C, T_d: 292 °C). Usually, the melting point of a compound has great relationship with the intermolecular and intramolecular interactions. ANFF-34 has three kinds of hydrogen bonds (N8–H8A···O2, N8–H8B···O5, N8–H8B···N3) while ANFF-43 has only two kinds (N8–H8A···N7, N8–H8B···N5). The structural differences result in different intermolecular and intramolecular interactions, which further lead to the melting point of ANFF-43 lower than that of ANFF-34. From the TG traces of these two compounds (Fig. 7), the weight loss process of ANFF-34 is slightly delayed compared to that of ANFF-43, and the residues of these two compounds are less than 5%, indicating nearly complete decomposition.

The thermal decomposition processes of ANFF-34 and ANFF-43 were further investigated using non-isothermal kinetic study and compared by Kissinger's method.[12] The DSC traces of ANFF-34 and ANFF-43 obtained at various heating rates (2.5, 5, 10 and 20 °C min^{-1}) are shown in Fig. 8 and 9. The decomposition peak temperatures of ANFF-34 at different heating rates are 208.3 °C, 204.1 °C, 212.7 °C and 222.4 °C. And the decomposition peak temperatures of ANFF-43 are 237.2 °C, 246.4 °C, 255.6 °C and 264.8 °C, respectively.

The apparent activation energy E_k of ANFF-34 at atmospheric pressure is 52.22 kJ mol^{-1}, which is close to that of DNTF[13] (58.8 kJ mol^{-1}). And the E_k of ANFF-43 is 142.1 kJ mol^{-1}, which is much higher than that of DNTF. The results indicate that both ANFF-34 and ANFF-43 have good thermal stability at atmospheric condition (Table 2).

Physiochemical and energetic properties of ANFF-34 and ANFF-43

The physiochemical and energetic properties of ANFF-34 and ANFF-43 are summarized in Table 3. For comparison, those of TNT and DNTF are also included. The gas-phase enthalpies of formation were calculated by quantum chemical method, and the enthalpies of sublimation were estimated based on the electrostatic potential parameters. The solid-state enthalpies of formation of ANFF-34 and ANFF-43 were obtained as 602.3 kJ mol^{-1} and 583.9 kJ mol^{-1}, respectively. Both ANFF-43 and ANFF-34 possess positive heats of formation, mainly owing to the high enthalpy of formation of furazan rings.

Based on the crystal densities and calculated heats of formation, the detonation performances of ANFF-34 and ANFF-43 were calculated. Among the two isomers, the molecular packing of ANFF-34 is relatively compact, with a crystal density of 1.80 g cm^{-3}, which is greater than that of ANFF-43 (1.70 g cm^{-3}). ANFF-34 possesses a detonation velocity of 8214 m s^{-1}, detonation pressure of 30.5 GPa, while ANFF-43 shows relatively lower performances (D: 7868 m s^{-1}, P: 27.0 GPa). The results verified that the different positions of the oxygen atoms on the furoxan rings result in different intramolecular and intermolecular hydrogen bonding, and directly

Table 3 The physicochemical properties and detonation performances of ANFF-34, ANFF-43, TNT, DNTF and BOM

Comp.	ANFF-34	ANFF-43	TNT	DNTF	BOM[13]
ρ^a (g cm^{-3})	1.802	1.700	1.65 (ref. 14)	1.937 (ref. 6)	1.832
$\Delta_f H^b$ (kJ mol^{-1})	602.3	583.9	−67	644.3	−79.4
$T_m{}^c$ (°C)	116.2	106.2	81	110 (ref. 7)	84.5
$T_d{}^d$ (°C)	255.4	255.6	295 (ref. 14)	292 (ref. 7)	183.4
Ω^e (%)	−39.7	−39.7	−74	−20.5	−33.3
D^f (m s^{-1})	8214	7868	6881 (ref. 14)	9250 (ref. 6)	8180
P^g (GPa)	30.5	27.0	19.5 (ref. 14)	41.1	29.4
IS^h (J)	>40	>40	15	26	8.6
FS^i (N)	>360	>360	240	240	282

[a] Density. [b] Heats of formation calculated by Gaussian 09.[15] [c] Melting temperature (endothermic peak). [d] Decomposition temperature (exothermic peak). [e] Oxygen balance (based on CO_2) for $C_aH_bO_cN_d$, $16(c-(2a+0.5b))$/MW, MW = molecular weight. [f] Calculated detonation velocity (EXPLO5 v 6.04). [g] Calculated detonation pressure (EXPLO5 v 6.04).[16] [h] Impact sensitivity evaluated by a standard BAM fall-hammer. [i] Friction sensitivity evaluated by BAM technique.[17]

affect the arrangement of molecules in the crystal, which finally lead to the significant differences in their performances. The sensitivities of ANFF-34 and ANFF-43 to impact are >40 J and to friction are >360 N. In comparison with DNTF, the mechanical sensitivities of these two derived compounds decreased after the introduction of amino groups.

Conclusions

In summary, two melt-cast explosives ANFF-34 (T_m: 116.2 °C, T_d: 255.4 °C) and ANFF-43 (T_m: 106.2 °C, T_d: 255.6 °C) were synthesized *via* a carefully controlled reaction strategy under low-temperature, with improved yields of 32% and 38%. For the first time, we unambiguously distinguished the structures of ANFF-34 and ANFF-43, by comparing the experimental and theoretical values of the chemical shifts of ^{15}N NMR. The X-ray single diffraction patterns indicate that ANFF-34 possesses a "face-to-face" dimer configuration through N–H···O bonds, while ANFF-43 exists as a "hand-in-hand" dimer configuration through N–H···N bonds. From the X-ray analysis, the densities of energetic compounds are closely related to intermolecular and intramolecular interactions. The closer three-dimensional packing of ANFF-34 leads to its higher packing density (1.8 g cm^{-3}), in comparison with that of ANFF-43 (1.7 g cm^{-3}). Hence, the detonation performances of ANFF-34 (D: 8214 m s^{-1}, P: 30.5 GPa) are better than those of ANFF-43 (D: 7868 m s^{-1}, P: 27.0 GPa). In addition, the impact sensitivities of ANFF-34 and ANFF-43 are >40 J and the friction sensitivities for them are >360 N, indicating their low sensitivities to impact and friction. By replacing one nitro group of DNTF with amino group, the two isomers ANFF-34 and ANFF-43 showed satisfactory thermal behaviours and reduced mechanical sensitivities, suggesting their great potential to be used as melt-cast explosives. We believe that this work provides a solid foundation for the design and synthesis of new energetic compounds through isomer effect, and will promote new explorations in this field.

Conflicts of interest

There are no conflicts to declare.

Acknowledgements

We are grateful to the financial support from National Natural Science Foundation of China (No. 21805223, No. 21805224).

Notes and references

1 P. Ravi, D. M. Badgujar, G. M. Gore, S. P. Tewari and A. K. Sikder, *Propellants, Explos., Pyrotech.*, 2011, **36**, 393; Z. Wang, J. G. Zhang, J. T. Wu and T. L. Zhang, *RSC Adv.*, 2016, **6**, 44742.

2 S. S. Novikov, L. I. Khmel'nitskii, O. V. Lebedev, V. V. Sevast'yanova and L. V. Epishina, *Khim. Geterotsikl. Soedin.*, 1970, **5**, 465; J. R. Cho, K. J. Kim, S. G. Cho and J. K. Kim, *J. Heterocycl. Chem.*, 2002, **39**, 141.

3 N. R. Smith and R. H. Wiley, *US Pat.* 3165753, Assignee: The United States of America as represented by the Secretary of the Navy, Washington, DC, USA, 1965; Y. X. Li, D. L. Cao and J. L. Wang, *Acta Armamentarii*, 2013, **34**, 36.

4 T. G. Archibald, R. Gilardi, K. Baum and C. George, *J. Org. Chem.*, 1990, **55**, 2920; A. R. Katrizky, D. J. Cundy and J. Chen, *J. Heterocycl. Chem.*, 1994, **31**, 271; N. Sikder, A. K. Sikder, N. R. Bulakh and B. R. Gandhe, *J. Hazard. Mater.*, 2004, **113**, 35.

5 Y. S. Zhou, B. Z. Wang, J. K. Li, C. Zhou, L. Hu, Z. Q. Chen and Z. Z. Zhang, *Acta Chim. Sin.*, 2011, **69**, 1673; R. Tsyshevsky, P. Pagoria, M. X. Zhang, A. Racoveanu, A. DeHope, D. Parrish and M. M. Kuklja, *J. Phys. Chem. C*, 2015, **119**, 3509.

6 F. Q. Zhao, P. Chen, R. Z. Hu, Y. Luo, Z. Z. Zhang, Y. S. Zhou, X. W. Yang, Y. Gao, S. L. Gao and Q. Z. Shi, *J. Hazard. Mater.*, 2004, **113**, 67; F. Q. Zhao, P. J. Guo, R. Z. Hu, H. Zhang, Z. M. Xia, H. X. Gao, P. Chen, Y. Luo, Z. Z. Zhang, Y. S. Zhou, H. A. Zhao, S. L. Gao, Q. Z. Shi, G. E. Lu and J. Y. Jiang, *Chin. J. Chem.*, 2006, **24**, 631.

7 R. Duddu, J. Hoare, P. Sanchez, R. Damavarapu and D. Parrish, *J. Heterocycl. Chem.*, 2017, **54**, 3087.

8 C. He, H. Gao, G. H. Imler, D. A. Parrish and J. M. Shreeve, *J. Mater. Chem. A*, 2018, **6**, 9391; J. Yuan, X. Long and C. Zhang, *J. Phys. Chem. A*, 2016, **120**, 9446.

9 L. J. Zhai, F. Q. Bi, Y. F. Luo, L. Sun, H. Huo, J. C. Zhang, J. J. Zhang, B. Z. Wang and S. P. Chen, *Chem. Eng. J.*, 2020, **391**, 123573; D. Fischer, T. M. KlapÖtke and J. Stierstorfer, *Eur. J. Inorg. Chem.*, 2014, **34**, 5808; C. L. He, Y. X. Tang, L. A. Mitchell, D. A. Parrish and J. M. Shreeve, *J. Mater. Chem. A*, 2016, **4**, 8969.

10 T. K. Kim, J. H. Choe, B. W. Lee and K. H. Chung, *Bull. Korean Chem. Soc.*, 2012, **33**, 2765.

11 M. A. Spackman and D. Jayatilaka, *CrystEngComm*, 2009, **11**, 19; M. A. Spackman and J. J. McKinnon, *CrystEngComm*, 2002, **4**, 378.

12 H. E. Kissinger, *Anal. Chem.*, 1957, **29**, 1702.

13 E. C. Johnson, J. J. Sabatini, D. E. Chavez, R. C. Sausa, E. C. Byrd, L. A. Wingard and P. E. Guzmàn, *Org. Process Res. Dev.*, 2018, **22**, 736; X. Yang, J. Zhou, X. L. Xing, Y. F. Huang, Z. F. Yan, Q. Xue, X. F. Wang and B. Z. Wang, *RSC Adv.*, 2020, **10**, 26425.

14 H. Huo, J. L. Zhang, J. Dong, L. J. Zhai, T. Guo, Z. J. Wang, F. Q. Bi and B. Z. Wang, *RSC Adv.*, 2020, **10**, 11816.

15 M. J. Frisch, G. W. Trucks, H. B. Schlegel, G. E. Scuseria, M. A. Robb, J. R. Cheeseman, J. A. Montgomery Jr, T. Vreven, K. N. Kudin, J. C. Burant, J. M. Millam, S. S. Iyengar, J. Tomasi, V. Barone, B. Mennucci, M. Cossi, G. Scalmani, N. Rega, G. A. Petersson, H. Nakatsuji, M. Hada, M. Ehara, K. Toyota, R. Fukuda, J. Hasegawa, M. Ishida, T. Nakajima, Y. Honda, O. Kitao, H. Nakai, M. Klene, X. Li, J. E. Knox, H. P. Hratchian, J. B. Cross, V. Bakken, C. Adamo, J. Jaramillo, R. Gomperts, R. E. Stratmann, O. Yazyev, A. J. Austin, R. Cammi, C. Pomelli, J. W. Ochterski, P. Y. Ayala, K. Morokuma, G. A. Voth, P. Sal-vador, J. J. Dannenberg, V. G. Zakrzewski, S. Dapprich, A. D. Daniels, M. C. Strain, O. Farkas,

D. K. Malick, A. D. Rabuck, K. Raghavachari, J. B. Foresman, J. V. Ortiz, Q. Cui, A. G. Ba-boul, S. Clifford, J. Cioslowski, B. B. Stefanov, G. Liu, A. Liashenko, P. Piskorz, I. Komaromi, R. L. Martin, D. J. Fox, T. Keith, M. A. Al-Laham, C. Y. Peng, A. Nanayakkara, M. Challacombe, P. M. W. Gill, B. Johnson, W. Chen, M. W. Wong, C. Gonzalez and J. A. Pople, *Gaussian 09, rev. A.02*, Gaussian, Inc., Wallingford, CT, 2009.

16 M. Suceska, *EXPLO5, Version 6.04*, 2017.

17 *Test methods according to the UN Recommendations on the Transport of Dangerous Goods, Manual of Tests and Criteria*, United Nations Publication, New York, 4th edn, 2003, 13.4.2 Test 3 (a) (ii) BAM Fall hammer, p. 75, 13.5.1 Test 3 (b) (i) BAM friction apparatus, p. 104.